*1170–1176* *Nucleic Acids Research, 2015, Vol. 43, No. 2* *Published online 24 December 2014*
*doi: 10.1093/nar/gku1335*

# Molecular crowding overcomes the destabilizing effects of mutations in a bacterial ribozyme

**Hui-Ting Lee[1], Duncan Kilburn[1,2], Reza Behrouzi[1], Robert M. Briber[3] and Sarah A. Woodson[1,*]**

[1]Thomas C. Jenkins Department of Biophysics, Johns Hopkins University, 3400 N. Charles Street, Baltimore, MD 21218, USA, [2]Center for Neutron Scattering Research, National Institute of Standards and Technology, 100 Bureau Dr., Gaithersburg, MD 20899, USA and [3]Department of Materials Science and Engineering, University of Maryland, College Park, MD 20742, USA

Received October 21, 2014; Revised December 1, 2014; Accepted December 5, 2014

## ABSTRACT

**The native structure of the *Azoarcus* group I ribozyme is stabilized by the cooperative formation of tertiary interactions between double helical domains. Thus, even single mutations that break this network of tertiary interactions reduce ribozyme activity in physiological $Mg^{2+}$ concentrations. Here, we report that molecular crowding comparable to that in the cell compensates for destabilizing mutations in the *Azoarcus* ribozyme. Small angle X-ray scattering, native polyacrylamide gel electrophoresis and activity assays were used to compare folding free energies in dilute and crowded solutions containing 18% PEG1000. Crowder molecules allowed the wild-type and mutant ribozymes to fold at similarly low $Mg^{2+}$ concentrations and stabilized the active structure of the mutant ribozymes under physiological conditions. This compensation helps explains why ribozyme mutations are often less deleterious in the cell than in the test tube. Nevertheless, crowding did not rescue the high fraction of folded but less active structures formed by double and triple mutants. We conclude that crowding broadens the fitness landscape by stabilizing compact RNA structures without improving the specificity of self-assembly.**

## INTRODUCTION

Many non-coding RNAs must fold into specific three-dimensional (3D) shapes to function in the cell (1–3). These 3D structures are defined by tertiary interaction motifs that hold double helices together and that contribute to the overall stability of the folded RNA (4–9). Using the group I ribozyme from the *Azoarcus* bacterium as a model system, we previously showed that tertiary interactions in different regions of the RNA form cooperatively during assembly of the core helices early in the folding process (10). This cooperative interaction network favors native-like intermediates and suppresses alternative, non-native conformations.

Because single mutations can disrupt this cooperative tertiary interaction network, they can substantially destabilize the native structure of the RNA and reduce its *in vitro* activity, as observed in a number of ribozymes (4,11–14). Consequently, many RNAs appear intolerant to mutation, raising the question of how non-coding RNAs evolve new functions or adapt to different genetic contexts. Nevertheless, previous studies on group I ribozymes showed that mutations in tertiary interaction motifs impaired the ribozyme much less in the cell than in the test tube (12,15–16). These observations suggested that the intracellular environment allows less stable sequences to fold, either by stabilizing the native tertiary structure or by reducing misfolding.

Here, we show that molecular crowding comparable to that in the cell overcomes the destabilizing effects of single, double or triple mutations that disrupt specific tertiary interactions in the *Azoarcus* group I ribozyme. In the crowded interior of a cell, macromolecules occupy ∼30% of the available volume and thus restrict the space available to an RNA molecule (17). Such excluded volume effects lower the translational and configurational entropy of the unfolded RNA more than they lower the entropy of the folded RNA, driving the folding equilibrium toward the native state.

We previously used small angle X-ray scattering (SAXS) to show that synthetic crowders such as polyethylene glycol (PEG) or Ficoll stabilize the folded structure of the wild-type (WT) ribozyme through excluded volume effects (18,19). By contrast, small co-solutes such as sucrose and ethylene glycol do not stabilize this ribozyme's tertiary

*To whom correspondence should be addressed. Tel: +410-516-2015; Fax: +410-516-4118; Email: swoodson@jhu.edu
Present addresses:
Hui-Ting Lee, Department of Bioengineering, University of Illinois, Urbana Champaign, Urbana IL 61801, USA.
Duncan Kilburn, Circulomics Inc., 810 Wyman Park Dr., Unit G01, Baltimore, MD 21211, USA.
Reza Behrouzi, Department of Cell Biology, Harvard Medical School, Boston, MA 02115-5730, USA.

structure (18,19). Here, we show that these excluded volume effects are sufficient to offset the loss of specific RNA tertiary interactions, so that mutant and WT ribozymes fold in similar $Mg^{2+}$ concentrations in a crowded solution. Molecular crowding also increases the ribozyme activity. Nevertheless, the double and triple mutants turnover more slowly than the WT RNA, because the mutants form both active and inactive structures. We conclude that crowding drives RNAs into compact structures in physiological $Mg^{2+}$ concentrations, but cannot improve the specificity of folding when tertiary interactions are lost. We discuss how specific and non-specific stabilization of RNA tertiary structure is likely to influence the natural selection of non-coding RNAs.

## MATERIALS AND METHODS

### RNA preparation

The *Azoarcus* group I L-9 and L-3 ribozymes (WT and mutants) were prepared by run-off T7 transcription and purified by polyacrylamide gel electrophoresis (PAGE) as previously described (10,20). The 9-nt RNA substrate 5′ rCAUAUCGCC was obtained from Integrated DNA Technologies. Final samples contained 0.4 mg/ml (6 μM) ribozyme in 20 mM Tris–HCl (pH 7.5), plus the stated concentrations of $MgCl_2$ and PEG 1000 at 37°C.

### Small angle X-ray scattering

SAXS measurements were conducted at BioCAT (ID18; Advanced Photon Source, Argonne National Laboratory, IL, USA) at wavelength = 1.033 Å (12 keV) over the momentum transfer range Q = 0.006–0.34 $Å^{-1}$. The SAXS data were corrected for background scattering and indirectly transformed to yield the pair distribution function, $P(r)$, and the radius of gyration, $R_g$ (21). RNA was refolded as previously described (10,18) except that diluted RNA in 20 mM Tris–HCl was incubated at 50°C for 5 min before and after the addition of PEG1000. Each sample (100 μl) was individually adjusted to the desired $MgCl_2$ concentration, then incubated 10 min at 50°C and 30 min at 37°C. This method of sample preparation may account for slightly smaller differences between the WT and particular mutant ribozymes than previously observed when the RNA was prefolded at 50°C and titrated in $MgCl_2$ at 37°C (10).

### Native PAGE

RNA samples were prepared as for SAXS, except samples were doped with a small amount of $^{32}$P-labeled RNA and contained 7% (v/v) glycerol and <0.1% (w/v) xylene cyanol. After equilibration at 37°C, samples were immediately loaded on a native 6% polyacrylamide gel as previously described (22).

### Ribozyme activity assay

Single-turnover cleavage assays were carried out at 37°C as previously described (23). L-3 ribozyme (6 μM) was refolded in the desired [$MgCl_2$] as for SAXS, but with 5 mM GTP. Reactions were started with the addition of ∼10 nM $^{32}$P-labeled RNA substrate and quenched after 25 s or 3 min by an equal volume of 30 mM ethylenediaminetetraacetic acid, 10 M urea and 0.1X Tris-borate EDTA on ice. Both the ribozyme and substrate were equilibrated with the same concentration of $PEG_{1000}$ at 37°C before mixing to eliminate any change in viscosity. Quenched reactions were analyzed by denaturing 20% PAGE and the fraction of product over time fit to a stretched exponential rate equation (see SI Methods). The slower rate of cleavage in 18% PEG can be accounted for by the change in the viscosity of the solution (19).

### Free energy calculations

Previous work showed that $R_g$ behaves as an order parameter of the solution and can be used to measure the fraction of folded and unfolded RNA (24). Footprinting results confirmed that the tertiary folding of the *Azoarcus* ribozyme is reasonably approximated by a two or three-state equilibrium (25,26). The change in $R_g$ as a function of $Mg^{2+}$ concentration $C$ was fit to a three-state model (27):

$$R_g^2(C) = \frac{R_{g,U}^2 + R_{g,Iu}^2(C/C_{m,1})^{n1} + R_{g,Ic}^2(C/C_{m,2})^{n2}}{1 + (C/C_{m,1})^{n1} + (C/C_{m,2})^{n2}} \quad (1)$$

in which $R_{g,U}$ and $R_{g,Ic}$ are directly determined from the SAXS data in the lowest and highest $Mg^{2+}$ concentrations and the other parameters are obtained from fits to the data. The fitted parameter values were used to simulate the population of $I_C$ (see SI Methods). The populations of $I_C$ and N (from activity assays) were fit to two-state transitions, $f(C) = C^n/(C_m{}^n + C^n)$, to give the midpoint $C_m$ and slope $n$ of each folding transition with and without $PEG_{1000}$. For each mutant, the free energies of the $I_U \rightarrow I_C$ and $I_C \rightarrow N$ folding transitions, $\Delta G(C) = -nRT\ln(C_{ref}/C_m)$, were evaluated at a reference concentration of $Mg^{2+}$ $C_{ref}$, which is equal to half-saturation of the corresponding WT folding transition in dilute buffer or 18% $PEG_{1000}$, respectively. The confidence intervals of fitted parameters were estimated by a bootstrapping method as previously described (10). The value and reported error of $C_m$, $n$ and $\Delta G$ were obtained from the mean and standard deviation of the bootstrapping results. The free energy perturbations due to the mutations were calculated from $\Delta\Delta G = \Delta G^{mut} - \Delta G^{WT}$ in each folding condition.

## RESULTS

### Folding of the *Azoarcus* ribozyme

For our experiments, we used the group I ribozyme from the purple bacterium *Azoarcus* sp. BH72, which has an unusually stable secondary and tertiary structure (Figure 1a and b) (28). The tertiary structure of the ribozyme folds in three macroscopic phase transitions (Figure 1c). In 0.2 mM $MgCl_2$, the ribozyme forms an extended intermediate ($I_U$) that is more compact and flexible than the unfolded RNA in no $MgCl_2$ (27,29). In 1 mM $MgCl_2$, the double helices assemble into a compact, native-like intermediate ($I_C$) that is readily detected by solution scattering (30) and native PAGE (22). Further rearrangement of the tertiary interactions in ≥3 mM $MgCl_2$ results in the active, native state (N)

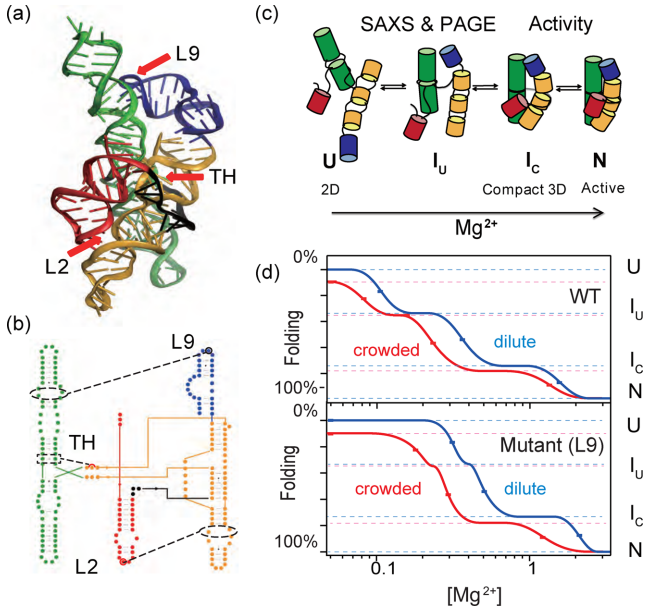


**Figure 1.** Molecular crowding stabilizes the folded *Azoarcus* ribozyme. (**a**,**b**) Tertiary and secondary structure (PDB 1U6B). Red arrows (a) and circles (b) indicate point mutations that disrupt tertiary interactions: L2 tetraloop, A25U; TH (triple helix), G125A; L9 tetraloop, A190U. (**c**) As $[Mg^{2+}]$ rises, the population shifts from an unfolded state (U) with secondary but no tertiary structure, to the extended intermediate ($I_U$), the native-like compact intermediate ($I_C$) and finally the native structure (N). (**d**) Landscape illustrating the $Mg^{2+}$-dependence of folding in dilute (blue) and crowded (red) solutions. Both RNAs fold at lower $[Mg^{2+}]$ in a crowded solution, but the L9 mutation changes the relative stabilities of $I_U$ and $I_C$. Midpoints of the U→$I_U$ and $I_U$→$I_C$ transitions were calculated from three-state fits to SAXS data. Midpoints of the $I_C$→N transition were obtained from the relative ribozyme activity (25 s). The degree of foldedness represented by the y-axis is arbitrary.

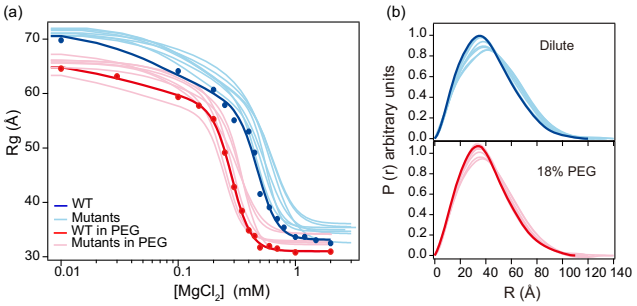


**Figure 2.** Molecular crowding overcomes destabilizing RNA mutations. Folding transitions from the unfolded state (U) to the compact native-like intermediate ($I_C$) were measured by SAXS at different $[Mg^{2+}]$. Filled symbols indicate experimental data on the WT ribozyme; lines show the best fit of the data to a 3-state partition function (Equation 1). Light lines indicate fitted transitions for one of the seven possible single, double or triple L2, TH and L9 mutants; see data in Supplementary Figure S3. No PEG, blue/light blue; 18% PEG1000, red/pink. All experiments were done with 0.4 mg/ml RNA equilibrated in 20 mM Tris–HCl, pH 7.5 plus the desired $[MgCl_2]$ at 37°C. (**b**) Normalized $P(r)$ of the folded RNAs in 2 mM $MgCl_2$ in water or in 18% $PEG_{1000}$. Colors as in (**a**).

that can be detected in biochemical assays (31,32). We used SAXS, native PAGE and ribozyme activity to distinguish the effects of crowding and mutations on each stage of folding (Figure 1d).

For this study, we measured the destabilization of the RNA structure owing to single base substitutions that disrupt a conserved triple helix (TH) in the center of the ribozyme core, or that disrupt docking of two peripheral L2 and L9 tetraloops with their respective helical receptor in P8/P8a and P5/P5a (Figure 1a and b). These comprise three of the main tertiary interaction motifs that stabilize the *Azoarcus* ribozyme. As previously demonstrated (10), ribozymes carrying single, double or triple combinations of these mutations were able to fold into a compact tertiary structure (Supplementary Figure S1) and were catalytically active in 15 mM $MgCl_2$ (Supplementary Figure S2). Because these mutations do not prevent the ribozyme from folding in high $Mg^{2+}$, we could evaluate how each mutation perturbed the equilibria between the U, $I_C$ and N conformational ensembles.

### Crowding compensates for missing RNA tertiary interactions

To test how much molecular crowding similar to that in the cell's interior can compensate for the loss of RNA tertiary interactions, we compared the folding of mutant and WT *Azoarcus* ribozymes in the presence or absence of PEG with an average 1000 Da molecular weight. PEG stabilizes the folded ribozyme primarily by excluded volume effects (18–20), and is advantageous for SAXS experiments because of its low X-ray scattering contrast with water.

We used SAXS to measure the effect of molecular crowding on the initial stage of folding in which the double helices assemble into a compact structure. As expected, all of the RNAs went through a cooperative folding transition from the unfolded ensemble (U) in no $Mg^{2+}$ ($R_g$ ~72 Å) to the compact $I_C$ intermediate in 1 mM $Mg^{2+}$ ($R_g$ = 32 Å; dark blue, Figure 2a). We also detected a decrease in $R_g$ at very low $Mg^{2+}$ that corresponds to formation of the extended intermediate, $I_U$. The change in $R_g^2$ was fit to a previously validated three-state model for folding (27) to obtain the equilibrium populations of U, $I_U$ and $I_C$ at each $Mg^{2+}$ concentration and the free energy gaps between these states (Supplementary Table S1).

In dilute buffer, the mutant ribozymes required more $Mg^{2+}$ to fold than the WT ribozyme, consistent with a less stable tertiary structure (compare dark and light blue curves in Figure 2a; see Supplementary Figure S3 for further data). The mutants also formed less compact structures than the WT ribozyme in 2–5 mM $MgCl_2$, as indicated by a greater $R_g$ and more asymmetric pair-distance distribution function $P(r)$ (Figure 2b). When 18% PEG1000 was added to the solution, all of the RNAs were stabilized. They folded at lower $Mg^{2+}$ concentrations (red; Figure 2a) and had more symmetric $P(r)$ functions (Figure 2b) in 2 mM $MgCl_2$, as previously observed for the WT *Azoarcus* ribozyme (20).

Importantly, PEG stabilized the mutant ribozymes more than the WT ribozyme, so that $[Mg^{2+}]_{1/2}$ for folding the WT ribozyme was near the average for the group (compare red and pink lines in Figure 2a). This result showed that the stabilization arising from a crowded environment compensates the loss of RNA tertiary interactions, equalizing the folding of the WT and mutant RNAs. This compensation was also

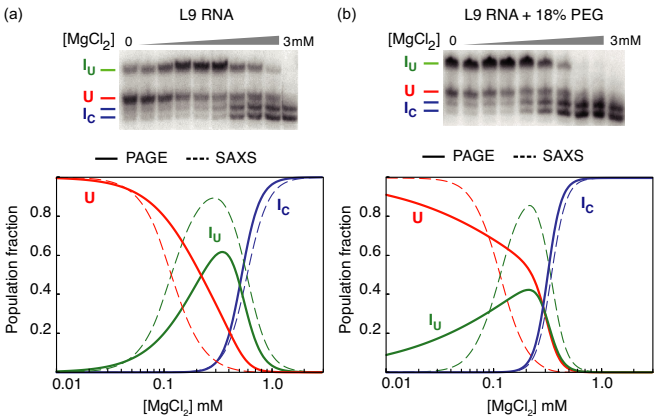


**Figure 3.** Crowding stabilizes native and non-native intermediates. Folding of the L9 mutant was analyzed by native PAGE in (**a**) dilute solution and (**b**) 18% $PEG_{1000}$. Top, native PAGE was performed in the same experimental condition as SAXS. Bands were assigned as described in SI Methods. The two high mobility bands have the same response to $[Mg^{2+}]$ and were grouped. Bottom, populations of each conformer in solution calculated from native PAGE (solid lines) and the change in $R_g$ (dashed lines). Some of the unfolded RNA in solution folds to $I_U$ or $I_C$ when the sample contacts the $MgCl_2$ in the gel running buffer. U, unfolded RNA (red); $I_U$, extended folding intermediates (green); $I_C$, compact intermediates (blue). Fitted parameters are the standard deviation from 2–3 trials. Data for L9 and other ribozymes are shown in Supplementary Figure S3.

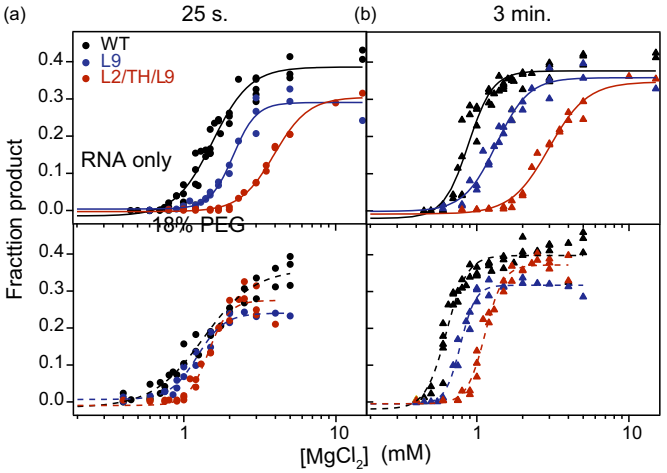


**Figure 4.** Crowding increases ribozyme activity. Formation of the native state (N) was measured in single-turnover activity assays (Supplementary Figure S4). The fraction of substrate cleaved versus $[Mg^{2+}]$ in three or more trials were fit to a two-state function. See Supplementary Figure S6 for further data on other mutants. (**a**) The product formed in 25 s indicates the fraction of native ribozyme at each $[Mg^{2+}]$. The mutants and WT fold similarly in 18% PEG, but the mutants have lower maximum activity. (**b**) Product formed in 3 min indicates the total population competent to react. PEG only partially compensates for destabilizing mutations in this assay, indicating a greater fraction of misfolded RNAs.

apparent from the similar *P(r)* functions of the WT and mutant RNAs folded in 18% PEG (Figure 2b).

## Crowding does not change the folding pathway

We next asked whether the *Azoarcus* ribozyme forms different intermediate structures in the crowded and dilute solutions, and whether this accounts for the stabilization by PEG. We used native PAGE to separate native-like and non-native intermediates, which have different electrophoretic mobility because of their different hydrodynamic shapes (see SI text). RNAs were folded with or without 18% PEG in the same conditions used for SAXS experiments (0.4 mg/ml RNA) and loaded on a native 8% polyacrylamide gel containing 3 mM $MgCl_2$ at 4°C.

Only the folded ($I_C$ + N) and the unfolded (U) conformations were observed for the WT ribozyme (22). We measured the folded and unfolded populations using a model that accounts for the fraction of RNA which folds as the sample is loaded into the gel (Supplementary Figure S1b). The increase in the folded population with $Mg^{2+}$ concentration coincided with the main folding transition measured by SAXS (Supplementary Figure S3a). This transition shifted to a lower $Mg^{2+}$ concentration in 18% PEG, in agreement with PEG's stabilization of compact structures.

In contrast to the WT ribozyme, the mutant ribozymes either migrated more slowly in the gel or formed additional bands corresponding to the extended $I_U$ intermediate and other non-native structures structures (Figure 3; see Supplementary Figure S1). For each ribozyme sequence, PEG increased the population of folded RNA but did not change the types of intermediates formed (Supplementary Figure S3b–h). We also observed that 18% PEG favored the $I_U$ state over the less compact U state, in low $Mg^{2+}$ (Figure 3b). This is consistent with the idea that crowding stabilizes the folded RNA by restricting the volume (and conformational space) available to the unfolded chains (18). These results also agreed with the suggestion that ions, crowders and other co-solutes change the relative stabilities of different conformations but not the folding pathways encoded by the RNA sequence (33–35).

## Molecular crowding stabilizes the native state

The results above showed that crowder molecules such as PEG offset the destabilizing effects of our ribozyme mutations, so that the mutant and WT RNAs form compact structures in comparable $Mg^{2+}$ concentrations. To determine whether the folded RNAs are active, we measured the amount of native ribozyme at different $Mg^{2+}$ concentrations using single-turnover RNA cleavage assays (36,37). In 15 mM $MgCl_2$, almost half the substrate was cleaved within 13–25 s at 37°C (Supplementary Figures S4 and S5). This is close to the maximal activity of the *Azoarcus* ribozyme (Supplementary Figure S2) and reflects the internal equilibrium between substrate cleavage and ligation (38). The amount of product formed in 25 s increased sharply between 1 and 3 mM $Mg^{2+}$ as the native ribozyme became more populated (Figure 4a).

The native states of the mutant ribozymes were less stable than the native WT ribozyme and required higher $Mg^{2+}$ concentration to form, as expected (Figure 4a and Supplementary Figure S6). The addition of 18% PEG shifted the titration curves for the mutants to lower $Mg^{2+}$, however, so that even the least active mutants (TH/L9 and L2/TH/L9) had the same $[Mg^{2+}]_{1/2}$ for forming the catalytically active native state as the WT ribozyme (Figure 4a and Supplementary Figure S6a). Therefore, a crowded environment not

only stabilizes the native ribozyme (19,39–40) but the WT and mutant ribozymes experience a similar free energy difference between the $I_C$ and N states.

### Crowding does not rescue misfolded ribozymes

Although PEG stabilized the compact ($I_C$) and native (N) states, certain ribozymes such as those containing the L9 mutation had a lower maximum activity than the WT ribozyme (Supplementary Figure S2). This reduced catalytic activity was consistent with the presence of an additional non-native conformer (Figure 3b) and some aggregation of the L9 mutant above 3 mM $Mg^{2+}$. PEG did not improve the maximum activity of such mutants, suggesting that molecular crowding cannot fully compensate for the loss of sequence-specific RNA interactions.

At low $Mg^{2+}$ concentrations, the initial phase of the substrate cleavage reaction requires up to 3 min (Supplementary Figure S7) (19). This slow cleavage rate is presumably because near-native ribozyme–substrate complexes only occasionally fluctuate into the reactive structure when the $Mg^{2+}$ concentration is too low to fully stabilize the ribozyme active site. The possibility of sampling suboptimal structures is supported by the observation that individual *Tetrahymena* group I ribozymes can react at different rates (41).

In the conditions tested here, the total fraction of ribozyme–substrate complexes capable of reaching the native state formed product within 3 min (Supplementary Figure S7). When this fraction of 'refoldable' RNA was compared at different [$MgCl_2$], the mutant ribozymes appeared less stable than the WT ribozyme in either dilute or crowded solutions (Figure 4b and Supplementary Figure S6b). In other words, PEG was less able to improve the activity of incorrectly folded RNA molecules that required more time to react. This result agreed with the inability of PEG to raise the maximum activity of mutants that readily form alternative structures, such as L9 or the least stable L2/TH/L9 triple mutant (Supplementary Figure S2 and S3). From these results, we concluded that a crowded environment stabilizes the native ribozyme structure in low $Mg^{2+}$, but cannot overcome the loss of folding specificity that arises when tertiary interaction motifs are mutated.

### Free energy landscape for folding in crowded solutions

To quantify the thermodynamic compensation for destabilizing RNA mutations, we compared the free energy change for forming the compact $I_C$ intermediate or the native (active) state in dilute solution and in 18% PEG. Individual $Mg^{2+}$ titrations were fit to two or three-state folding models to obtain the populations of U, $I_U$ and $I_C$ (SAXS) and N (activity). These populations were used to calculate the standard free energy change ($\Delta G$) associated with the U to $I_C$ and $I_C$ to N folding transitions (SI Methods) (10). The energy perturbations caused by the mutations, $\Delta\Delta G = \Delta G^{mut} - \Delta G^{WT}$, were evaluated at the $MgCl_2$ concentration corresponding to 50% saturation of the WT folding transition in each solution condition. This choice of reference condition avoids extrapolation to $Mg^{2+}$ concentrations where the assumptions underlying the thermodynamic model are less valid (42).

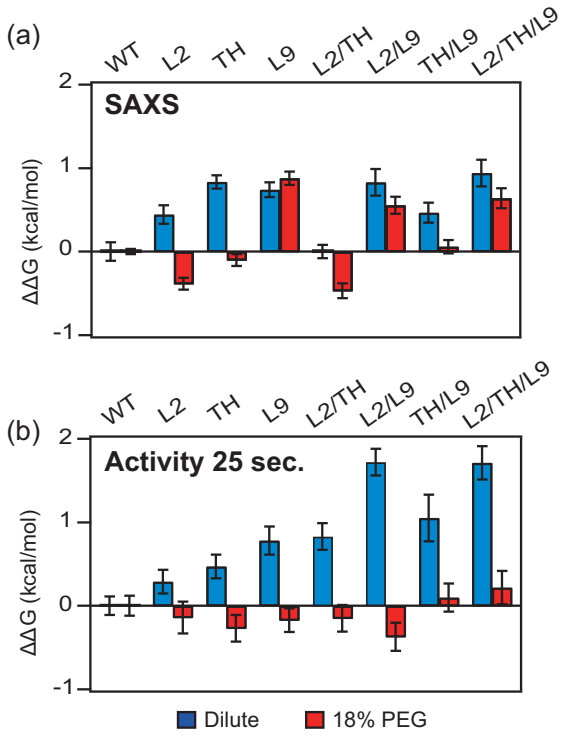


**Figure 5.** Crowding stabilizes the folded ribozymes. Relative folding free energies $\Delta\Delta G = \Delta G^{mut} - \Delta G^{WT}$ for (**a**) U→$I_C$ transition measured by SAXS and (**b**) the $I_C$→N transition measured by activity (25 s). The folding free energies were evaluated at $[Mg^{2+}]_{1/2}$ for the WT ribozyme in each solution condition: 0.47 mM $MgCl_2$ (SAXS, dilute), 0.28 mM (SAXS, 18% PEG), 1.56 mM (activity, dilute) and 1.34 mM $MgCl_2$ (activity, 18% PEG). Error bars depict the standard deviation calculated from 10 000 resampling of fit residuals. The free energy obtained from activity assay is normalized to maximum activity of each RNA (Supplementary Figure S2). The $[Mg^{2+}]_{1/2}$ values of the WT and single mutant ribozymes reported here are lower than previously reported (10), owing to the 25 s quench used here, versus <20 s quench used previously. The longer reaction interval allows a portion of semi-native intermediates to refold, boosting the relative activity of the WT ribozyme and making the relative effects of multiple mutations more apparent (Supplementary Figure S7).

All of the mutations destabilized the compact $I_C$ intermediate in dilute buffer, resulting in positive values for $\Delta\Delta G_{U\rightarrow IC}$ (blue bars, Figure 5a; Supplementary Table S1). These energy perturbations followed the same order as reported previously (10), but with a smaller magnitude. In 18% PEG, however, several mutants had a similar folding free energy as the WT ribozyme, and L2 and L2/TH even appeared more stable than the WT RNA (red bars; Figure 5a).

PEG also lowered the standard free energy change of the $I_c$→N transition calculated from the amount of product formed after 25 s. In dilute solution, the native state became progressively less stable ($\Delta\Delta G_{IC\rightarrow N} > 0$) as more tertiary interaction motifs were mutated. By contrast, the folding free energies of all ribozymes were very similar in 18% PEG (Figure 5b), again demonstrating that crowded environments can compensate for the loss of tertiary interactions outside the active site. As discussed above, crowding does not rescue near-native or non-native structures that re-

quire more time to fluctuate into the active state and react (Supplementary Figure S8).

## DISCUSSION

Molecular crowding favors the compact conformation of the *Azoarcus* ribozyme, allowing WT and mutant RNAs to fold into native-like structures in low physiological $Mg^{2+}$ concentrations. The similar folding free energies of the mutants tested here suggests that non-coding RNA structures can tolerate sequence changes during evolution better than predicted by *in vitro* folding assays. For example, some destabilizing mutations in the *td* group I ribozyme harmed intracellular self-splicing much less than expected (12). Recent work on the CPEB3 ribozyme suggests that stabilization from molecular crowding is particularly important for marginally stable RNA structures (40), but is observed for a variety of RNA structures (39,43–44).

We previously found that the cooperative formation of tertiary interactions during helix assembly makes folding more accurate because only native-like structures enjoy the additional drop in free energy that arises when multiple tertiary interactions form simultaneously (10). This cooperativity is most important when solvent conditions (such as low $[Mg^{2+}]$) barely stabilize the native state (45,46). By contrast, strongly stabilizing conditions diminish the selectivity of folding.

By non-selectively tilting the free energy landscape toward compact structures, molecular crowding allows the WT and mutant ribozymes an equal chance of accessing the native state without improving the precision of self-assembly. Instead, a crowded environment produces a broad basin of attraction that favors a variety of compact structures. Our SAXS, native PAGE and activity measurements all indicate that the mutated ribozymes sample folded conformations that are inactive in substrate cleavage assays, and this less-active fraction increases with the number of mutations with or without PEG (Supplementary Figure S6). Thus, our results show that molecular crowding does not overcome the loss of folding specificity that arises when one or more tertiary interaction motifs are lost.

One prediction of these results is that non-coding RNAs that act catalytically in the cell will be more sensitive to destabilizing mutations than non-coding RNAs that turnover only once, such as the *Azoarcus* group I ribozyme. Estimates of intracellular splicing rates suggest that a precursor RNA has 1–2 min to fold and react before it is degraded (47–50), so that even suboptimal sequences may succeed by this measure. By contrast, sequence changes that destabilize multiple turnover ribozymes such as RNase P (51) must presumably be accompanied by the evolution of other RNA or RNA–protein interactions that specifically reinforce the optimal RNA structure. Since other polymers stabilize the folded RNA as well as PEG does, generic excluded volume effects might have even boosted the functions of RNA catalysts in a pre-biotic world.

## SUPPLEMENTARY DATA

Supplementary Data are available at NAR Online.


## ACKNOWLEDGEMENTS

The authors thank Rita Graceffa and Srinivas Chakravarthy (APS ID18 BioCAT) for assistance with SAXS experiments. Use of the Advanced Photon Source, Argonne National Laboratory was supported by the U.S. Department of Energy, Office of Science, Office of Basic Energy Sciences, under Contracts Nos. DE-AC02-06CH11357.

## FUNDING

National Institute of General Medical Sciences [R01 GM60819]; National Institute of Standards and Technology [70NANB10H257]. The open access publication charge for this paper has been waived by Oxford University Press—*NAR* Editorial Board members are entitled to one free paper per year in recognition of their work on behalf of the journal.

*Conflict of interest statement.* None declared.


## REFERENCES


1. Holbrook,S.R. (2008) Structural principles from large RNAs. *Annu. Rev. Biophys.*, **37**, 445–464.
2. Butcher,S.E. and Pyle,A.M. (2011) The molecular interactions that stabilize RNA tertiary structure: RNA motifs, patterns, and networks. *Acc. Chem. Res.*, **44**, 1302–1311.
3. Cruz,J.A. and Westhof,E. (2009) The dynamic landscapes of RNA architecture. *Cell*, **136**, 604–609.
4. Baird,N.J., Srividya,N., Krasilnikov,A.S., Mondragon,A., Sosnick,T.R. and Pan,T. (2006) Structural basis for altering the stability of homologous RNAs from a mesophilic and a thermophilic bacterium. *RNA*, **12**, 598–606.
5. Jaeger,L., Michel,F. and Westhof,E. (1994) Involvement of a GNRA tetraloop in long-range RNA tertiary interactions. *J. Mol. Biol.*, **236**, 1271–1276.
6. Silverman,S.K. and Cech,T.R. (1999) Energetics and cooperativity of tertiary hydrogen bonds in RNA structure. *Biochemistry*, **38**, 8691–8702.
7. Doherty,E.A., Herschlag,D. and Doudna,J.A. (1999) Assembly of an exceptionally stable RNA tertiary interface in a group I ribozyme. *Biochemistry*, **38**, 2982–2990.
8. Costa,M. and Michel,F. (1995) Frequent use of the same tertiary motif by self-folding RNAs. *EMBO J.*, **14**, 1276–1285.
9. Shi,X., Bisaria,N., Benz-Moy,T.L., Bonilla,S., Pavlichin,D.S. and Herschlag,D. (2014) Roles of long-range tertiary interactions in limiting dynamics of the Tetrahymena group I ribozyme. *J. Am. Chem. Soc.*, **136**, 6643–6648.
10. Behrouzi,R., Roh,J.H., Kilburn,D., Briber,R.M. and Woodson,S.A. (2012) Cooperative tertiary interaction network guides RNA folding. *Cell*, **149**, 348–357.
11. Wilson,T.J., Zhao,Z.Y., Maxwell,K., Kontogiannis,L. and Lilley,D.M. (2001) Importance of specific nucleotides in the folding of the natural form of the hairpin ribozyme. *Biochemistry*, **40**, 2291–2302.
12. Brion,P., Michel,F., Schroeder,R. and Westhof,E. (1999) Analysis of the cooperative thermal unfolding of the td intron of bacteriophage T4. *Nucleic Acids Res.*, **27**, 2494–2502.
13. McDowell,S.E., Jun,J.M. and Walter,N.G. (2010) Long-range tertiary interactions in single hammerhead ribozymes bias motional sampling toward catalytically active conformations. *RNA*, **16**, 2414–2426.
14. Tanner,M.A., Anderson,E.M., Gutell,R.R. and Cech,T.R. (1997) Mutagenesis and comparative sequence analysis of a base triple joining the two domains of group I ribozymes. *RNA*, **3**, 1037–1051.
15. Nikolcheva,T. and Woodson,S.A. (1999) Facilitation of group I splicing in vivo: misfolding of the Tetrahymena IVS and the role of ribosomal RNA exons. *J. Mol. Biol.*, **292**, 557–567.
16. Donahue,C.P., Yadava,R.S., Nesbitt,S.M. and Fedor,M.J. (2000) The kinetic mechanism of the hairpin ribozyme in vivo: influence of RNA

helix stability on intracellular cleavage kinetics. *J. Mol. Biol.*, **295**, 693–707.
17. Ellis,R.J. (2001) Macromolecular crowding: obvious but underappreciated. *Trends Biochem. Sci.*, **26**, 597–604.
18. Kilburn,D., Roh,J.H., Behrouzi,R., Briber,R.M. and Woodson,S.A. (2013) Crowders perturb the entropy of RNA energy landscapes to favor folding. *J. Am. Chem. Soc.*, **135**, 10055–10063.
19. Desai,R., Kilburn,D., Lee,H.T. and Woodson,S.A. (2014) Increased ribozyme activity in crowded solutions. *J. Biol. Chem.*, **289**, 2972–2977.
20. Kilburn,D., Roh,J.H., Guo,L., Briber,R.M. and Woodson,S.A. (2010) Molecular crowding stabilizes folded RNA structure by the excluded volume effect. *J. Am. Chem. Soc.*, **132**, 8690–8696.
21. Svergun,D.I. (1992) Determination of the regularization parameter in indirect- transform methods using perceptual criteria. *J. Appl. Crystallogr.*, **25**, 495–503.
22. Rangan,P., Masquida,B., Westhof,E. and Woodson,S.A. (2003) Assembly of core helices and rapid tertiary folding of a small bacterial group I ribozyme. *Proc. Natl. Acad. Sci. U.S.A.*, **100**, 1574–1579.
23. Chauhan,S., Behrouzi,R., Rangan,P. and Woodson,S.A. (2009) Structural rearrangements linked to global folding pathways of the Azoarcus group I ribozyme. *J. Mol. Biol.*, **386**, 1167–1178.
24. Fang,X., Littrell,K., Yang,X.J., Henderson,S.J., Siefert,S., Thiyagarajan,P., Pan,T. and Sosnick,T.R. (2000) Mg2+-dependent compaction and folding of yeast tRNAPhe and the catalytic domain of the B. subtilis RNase P RNA determined by small-angle X-ray scattering. *Biochemistry*, **39**, 11107–11113.
25. Chauhan,S., Caliskan,G., Briber,R.M., Perez-Salas,U., Rangan,P., Thirumalai,D. and Woodson,S.A. (2005) RNA tertiary interactions mediate native collapse of a bacterial group I ribozyme. *J. Mol. Biol.*, **353**, 1199–1209.
26. Chauhan,S. and Woodson,S.A. (2008) Tertiary interactions determine the accuracy of RNA folding. *J. Am. Chem. Soc.*, **130**, 1296–1303.
27. Moghaddam,S., Caliskan,G., Chauhan,S., Hyeon,C., Briber,R.M., Thirumalai,D. and Woodson,S.A. (2009) Metal ion dependence of cooperative collapse transitions in RNA. *J. Mol. Biol.*, **393**, 753–764.
28. Tanner,M. and Cech,T. (1996) Activity and thermostability of the small self-splicing group I intron in the pre-tRNA(lle) of the purple bacterium Azoarcus. *RNA*, **2**, 74–83.
29. Roh,J.H., Guo,L., Kilburn,J.D., Briber,R.M., Irving,T. and Woodson,S.A. (2010) Multistage collapse of a bacterial ribozyme observed by time-resolved small-angle X-ray scattering. *J. Am. Chem. Soc.*, **132**, 10148–10154.
30. Perez-Salas,U.A., Rangan,P., Krueger,S., Briber,R.M., Thirumalai,D. and Woodson,S.A. (2004) Compaction of a bacterial group I ribozyme coincides with the assembly of core helices. *Biochemistry*, **43**, 1746–1753.
31. Rangan,P. and Woodson,S.A. (2003) Structural requirement for Mg2+ binding in the group I intron core. *J. Mol. Biol.*, **329**, 229–238.
32. Rangan,P., Masquida,B., Westhof,E. and Woodson,S.A. (2004) Architecture and folding mechanism of the Azoarcus Group I Pre-tRNA. *J. Mol. Biol.*, **339**, 41–51.
33. Baird,N.J., Gong,H., Zaheer,S.S., Freed,K.F., Pan,T. and Sosnick,T.R. (2010) Extended structures in RNA folding intermediates are due to nonnative interactions rather than electrostatic repulsion. *J. Mol. Biol.*, **397**, 1298–1306.
34. Laederach,A., Shcherbakova,I., Jonikas,M.A., Altman,R.B. and Brenowitz,M. (2007) Distinct contribution of electrostatics, initial conformational ensemble, and macromolecular stability in RNA folding. *Proc. Natl. Acad. Sci. U.S.A.*, **104**, 7045–7050.
35. Rook,M.S., Treiber,D.K. and Williamson,J.R. (1998) Fast folding mutants of the Tetrahymena group I ribozyme reveal a rugged folding energy landscape. *J. Mol. Biol.*, **281**, 609–620.
36. Herschlag,D. and Cech,T.R. (1990) Catalysis of RNA cleavage by the Tetrahymena thermophila ribozyme. 1. Kinetic description of the reaction of an RNA substrate complementary to the active site. *Biochemistry*, **29**, 10159–10171.
37. Sinan,S., Yuan,X. and Russell,R. (2011) The Azoarcus group I intron ribozyme misfolds and is accelerated for refolding by ATP-dependent RNA chaperone proteins. *J. Biol. Chem.*, **286**, 37304–37312.
38. Wan,Y., Mitchell,D. 3rd and Russell,R. (2009) Catalytic activity as a probe of native RNA folding. *Methods Enzymol.*, **468**, 195–218.
39. Nakano,S., Karimata,H.T., Kitagawa,Y. and Sugimoto,N. (2009) Facilitation of RNA enzyme activity in the molecular crowding media of cosolutes. *J. Am. Chem. Soc.*, **131**, 16881–16888.
40. Strulson,C.A., Yennawar,N.H., Rambo,R.P. and Bevilacqua,P.C. (2013) Molecular crowding favors reactivity of a human ribozyme under physiological ionic conditions. *Biochemistry*, **52**, 8187–8197.
41. Solomatin,S.V., Greenfeld,M., Chu,S. and Herschlag,D. (2010) Multiple native states reveal persistent ruggedness of an RNA folding landscape. *Nature*, **463**, 681–684.
42. Leipply,D. and Draper,D.E. (2010) Dependence of RNA tertiary structural stability on Mg2 +concentration: interpretation of the Hill equation and coefficient. *Biochemistry*, **49**, 1843–1853.
43. Paudel,B.P. and Rueda,D. (2014) Molecular Crowding Accelerates Ribozyme Docking and Catalysis.J. Am. Chem. Soc., **136** , 16700 –16703.
44. Dupuis,N.F., Holmstrom,E.D. and Nesbitt,D.J. (2014) Molecular-crowding effects on single-molecule RNA folding/unfolding thermodynamics and kinetics. *Proc. Natl. Acad. Sci. U.S.A.*, **111**, 8464–8469.
45. Rook,M.S., Treiber,D.K. and Williamson,J.R. (1999) An optimal Mg(2+) concentration for kinetic folding of the tetrahymena ribozyme. *Proc. Natl. Acad. Sci. U.S.A.*, **96**, 12471–12476.
46. Thirumalai,D. and Woodson,S.A. (2000) Maximizing RNA folding rates: a balancing act. *RNA*, **6**, 790–794.
47. Koduvayur,S.P. and Woodson,S.A. (2004) Intracellular folding of the Tetrahymena group I intron depends on exon sequence and promoter choice. *RNA*, **10**, 1526–1532.
48. Roberts,G.C., Gooding,C., Mak,H.Y., Proudfoot,N.J. and Smith,C.W. (1998) Co-transcriptional commitment to alternative splice site selection. *Nucleic Acids Res.*, **26**, 5568–5572.
49. Donahue,C.P. and Fedor,M.J. (1997) Kinetics of hairpin ribozyme cleavage in yeast. *RNA*, **3**, 961–973.
50. Hilleren,P.J. and Parker,R. (2003) Cytoplasmic degradation of splice-defective pre-mRNAs and intermediates. *Mol. cell*, **12**, 1453–1465.
51. Walker,S.C. and Engelke,D.R. (2006) Ribonuclease P: the evolution of an ancient RNA enzyme. *Crit. Rev. Biochem. Mol. Biol.*, **41**, 77–102.